Detection of 2,4-Dinitrotoluene (DNT) as a Model System for Nitroaromatic Compounds via Molecularly Imprinted Short-Alkyl-Chain SAMs

ARTICLE *in* LANGMUIR · JUNE 2011

Impact Factor: 4.46 · DOI: 10.1021/la105128q · Source: PubMed

4 AUTHORS, INCLUDING:

Dahlia C. Apodaca
Mines and Geosciences Bureau
9 PUBLICATIONS **122** CITATIONS
SEE PROFILE

Roderick B Pernites
University of Houston
30 PUBLICATIONS **548** CITATIONS
SEE PROFILE

Rigoberto C. Advincula
Case Western Reserve University
334 PUBLICATIONS **7,240** CITATIONS
SEE PROFILE

Langmuir

ARTICLE

pubs.acs.org/Langmuir

Detection of 2,4-Dinitrotoluene (DNT) as a Model System for Nitroaromatic Compounds via Molecularly Imprinted Short-Alkyl-Chain SAMs

Dahlia C. Apodaca,[†,‡] Roderick B. Pernites,[†] Florian R. Del Mundo,[‡] and Rigoberto C. Advincula*[,†,‡]

[†]Department of Chemistry and Department of Chemical and Biomolecular Engineering, University of Houston, Houston, Texas 77204-5003, United States

[‡]Institute of Chemistry, University of the Philippines, Diliman, Quezon City, Philippines 1101

Supporting Information

ABSTRACT:

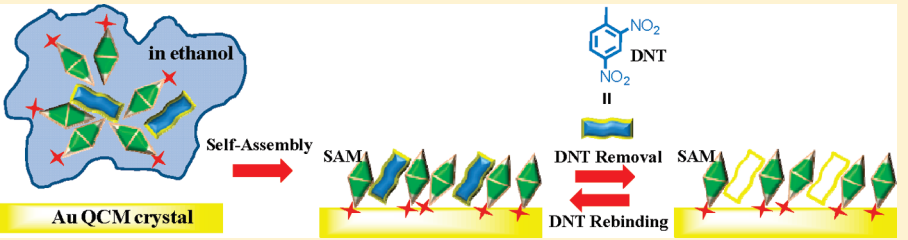

A 2-D molecularly imprinted monolayer (2-D MIM) approach was used to prepare a simple and robust sensor for nitroaromatic compounds with 2,4-dinitrotoluene (DNT) as the model compound, which is a precursor and analog for explosive 2,4,6-trinitrotoluene (TNT). In contrast to studies utilizing long-chain hexadecylmercaptan self-assembled monolayers (SAM)s for sensing, a shorter-chain alkylthiol (i.e., butanethiol SAM) was utilized for DNT detection. The role of the chain length of the coadsorbed alkylthiol was emphasized with a matched template during solution adsorption. Semiempirical PM3 quantum calculations were used to determine the molecular conformation and complexation of the adsorbates. A switching mechanism was invoked on the basis of the ability of the template analyte to alter the packing arrangement of the alkylthiol SAMs near defect sites as influenced by the DNT−ethanol solvent complex. A 2-D MIM was formed on the Au surface electrode of a quartz crystal microbalance (QCM), which was then used to sense various concentrations of the analyte. Interestingly, the 2-D MIM QCM also enabled the selective detection of DNT even in a mixed solution of competing molecules, demonstrating the selectivity figure of merit. Likewise, electrochemical impedance spectroscopy (EIS) data at different concentrations of DNT confirmed the 2-D MIM effectiveness for sensing based on the interfacial conformation and electron-transport properties of the imprinted butanethiol SAM.

INTRODUCTION

Sensor researchers and technologists are in a race to develop a robust sensor for detecting nitroaromatic compound-based high explosives not only in the vapor phase but also in aqueous solutions. Because of its potential harm as a concealed weapon, 2,4,6-trinitrotoluene (TNT) has become a target analyte of high interest for chemical sensor devices including its precursor, the one-nitro-group-less analog, 2,4-dinitrotoluene (DNT) (Figure 1). Edmiston et al.[1] described the ideal characteristics of a successful chemical sensor for TNT. It must be (1) extremely sensitive given that the vapor pressure of TNT at 25 °C is 5.8×10^{-6} Torr. The concentration of saturated TNT vapor in air at room temperature is known to be 5 ppb whereas that of DNT is in the range between 100 and 120 ppb.[2] It must be (2) highly selective, eliminating both false positives and false negatives; (3) robust and not prone to drift; and (4) have the ability to be easily miniaturized for field applications. Currently, most of the sensors for nitroaromatic compounds, though exhibiting high sensitivity, suffer from poor selectivity. Hence, effort is directed toward the development of future sensing devices consolidating good selectivity, fast speed, simplicity, and cost effectiveness with high sensitivity.[3] In particular, recent developments, in line with the fabrication of sensors for nitroaromatic compounds, involved the fabrication of a cross-reactive sensor array.[4] This is a collection of sensory materials that contains nonspecific sensors with chemical diversity so that the array differentially responds to different analytes. This approach eliminates the demand for highly selective sensors and considers only some of the sensors' important properties such as reproducibility and stability. To this end, research endeavoring to deal with the synthesis of detection schemes for the different nitroaromatic compounds may also contribute significant information for the development of this type of cross-reactive sensor array.

Received: December 29, 2010
Revised: April 20, 2011

   dx.doi.org/10.1021/la105128q | *Langmuir* XXXX, XXX, 000–000

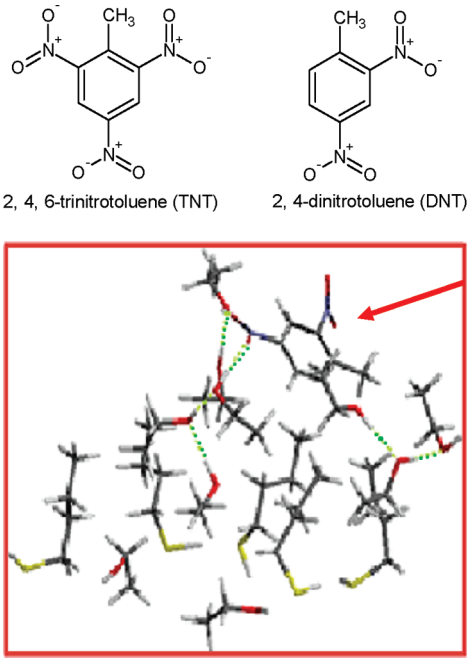

Figure 1. Structures of TNT and DNT nitroaromatic compounds and predicted conformation of butanethiol molecules across the monolayer film in ethanol in the presence of DNT as obtained through semiempirical PM3 calculations.

Molecular imprinting polymerization (MIP) has been used as a route to generate selective matrices for the detection and purification of chemical compounds.[5] Briefly, molecularly imprinted polymers are prepared by first combining the template and monomer(s) from a stable prepolymerization complex in a suitable solvent. In general, incorporating MIP with sensor technology is not as simple as it seems. For device sensing, the MIP as a recognition element must be interfaced effectively with the transducer. These transducers are often flat surfaces or electrodes, which enable high sensitivity based on changes in the electrical, optical, dielectric, or impedance properties of the surface.

A method to improve the sensitivity of MIP-based chemical sensors is to chemically modify a surface with organic molecule adsorbates.[6] Self-assembled monolayers (SAMs) are widely known to provide uniformly structured surfaces and allow the incorporation of functional groups that alter the surface's wetting,[7] frictional,[8] adhesive,[9] or recognition[10] properties. Examples include organothiols on metal (gold, silver, and copper) and organosilanes, organophosphates, and acids on metal oxide (ITO, alumina, and steel) substrates.[11] As thin film organic materials, they have been the subject of interest for a number of reasons: (1) SAMs are easy to generate from either solution or the gas phase; (2) they can be densely packed and precisely oriented; and (3) the thickness and the surface properties of the films can be monitored and adjusted. Alkanethiols on gold is the most extensively studied among SAMs.[12] The reaction may be considered to be an oxidative addition of the S−H bond to the gold surface, followed by reductive elimination of the H. The bonding of the thiolate group to the gold surface is very strong, with a homolytic bond strength of approximately 40 kcal/mol.[13]

The formation of thiol-based SAMs around a specific template on gold surfaces has been categorized as a type of 2-D imprinting technique.[14] There have been reports on the application of this principle to the preparation of 2-D chemical receptors.[15−19] However, some of these studies did not give a selectivity figure of merit for the sensor (i.e., did not demonstrate a preference toward a particular target molecule present in a mixture of other compounds). Also, a disadvantage of 2-D imprinting is the lack of stability of a non-cross-linked film brought about by the lateral diffusion of molecules, which usually occurs after the template extraction process.[13] Different transduction techniques have also been employed to monitor the binding of target analytes with these 2-D chemical receptors such as the capacitance technique employed by Mirsky et al.[20] in measuring the amount of bound barbituric acid in a 2-D dodecanethiol molecularly imprinted monolayer (MIM). On the other hand, Huan et al.[10] employed chronoamperometry for the rapid electrochemical sensing of nitrobenzene using a combined 2-D imprinting technique—the electropolymerization of self-assembled *o*-aminothiophenol species. Li and Husson[21] used surface plasmon resonance (SPR) spectroscopy to measure the adsorption of dansylated amino acids on the MIM surface prepared via a two-step imprinting process (i.e., pretreatment of the gold surface with a solution of the template followed by backfilling with thiol). Bi and Yang[22] presented the feasibility of using an MIM quartz crystal microbalance (QCM) to detect and differentiate two closely related neonicotinoids: imidacloprid and thiacloprid. On considering the latter two approaches, no detailed information was given pertaining to the mode of molecular interaction on the gold substrate with the templates used during the first step of the imprinting process or the so-called equilibrium deposition of templates.

In view of the foregoing discussions, it should be possible to exploit the recognition function of alkanethiol-based MIMs on DNT (Figure 1) by (1) establishing the QCM responses of different alkylthiol chain lengths in the presence of DNT; (2) differentiating the viscoelastic behavior of the DNT-imprinted butanethiol layer from a nonimprinted film; (3) demonstrating the kinetics of DNT binding (in solution) to the 2-D butanethiol monolayer; (4) investigating the selectivity behavior of the butanethiol MIP in a mixture of competing molecules; (5) characterizing the interfacial properties of both the imprinted and nonimprinted monolayer (NIM) butanethiol layer using the Faradaic electrochemical impedance spectroscopic technique (EIS); and (6) describing the monolayer film properties and nanostructure in the presence of the template through polarization modulation infrared reflectance absorption spectroscopy (PM-IRRAS), X-ray photoelectron spectroscopy (XPS), and ellipsometry. In principle, the adsorbed alkanethiol SAM serves as the main chemical recognition element directly interfaced with QCM transduction, enabling the quantification of the frequency shift and the motional resistance response. This should also allow in situ monitoring of the binding kinetics associated with adsorption of DNT on the 2-D MIM-modified gold electrode. Thus, the mass and viscoelastic behavior of the film can be monitored simultaneously during the rebinding process. Interestingly, to our knowledge the EIS technique has not been widely utilized to characterize the interfacial/charge-transfer phenomenon occurring at the alkylthiol SAM-modified electrode surface during template rebinding. Particular consideration is focused on establishing the influence of 2,4-DNT on the formation of butanethiol MIM on the gold surface. This is significant in controlling the molecular architecture at the electrode−solution interface for sensing applications. Optimization of the resolution

dx.doi.org/10.1021/la105128q |*Langmuir* XXXX, XXX, 000–000

Scheme 1. Fabrication of a 2-D DNT/QCM Sensor Using a Molecularly Imprinted SAM

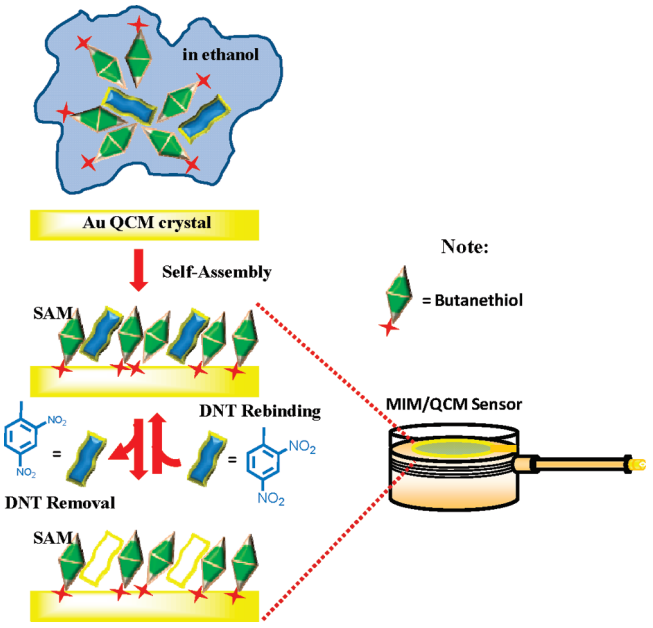

and detection of nitroaromatic compounds using alkanethiol self-assembled monolayers will be facilitated.

EXPERIMENTAL SECTION

Chemicals. 2,4-Dinitrotoluene (DNT), tetrabutylammonium hexafluorophosphate (TBAH), 2,4-dinitrophenol, 4-nitrotoluene and 2,6-dinitrotoluene were purchased from Sigma-Aldrich. All chemicals were used as received unless otherwise specified. Aqueous solutions were prepared from water purified using a Millipore system (resistivity 18.2 MΩ·cm).

Preparation of DNT-Imprinted Butanethiol MIM. Ethanol solutions of DNT and butanethiol were prepared with concentrations of 5 mM and 1% w/v, respectively. The concentration for the template reported by Piletsky et al.[18] was similarly used in this study. The imprinted monolayer film was prepared by the simultaneous coadsorption of DNT and butanethiol onto a cleaned gold surface via solution immersion (Scheme 1). For QCM sensing, the monolayer films were deposited on the gold surface of quartz crystals whereas samples for thickness by ellipsometry measurements and EIS sensing were deposited onto glass (2.5 × 1.5 cm^2) surfaces coated with gold (100 nm). Immersion was done overnight (12−20 h) at room temperature to ensure equilibrium binding of the molecules to the gold surface. The thiol-functionalized gold surfaces were washed repeatedly with fresh ethanol, including immersion over a period of 3 h on fresh ethanol to remove DNT and then blown dry with nitrogen. The same procedure was performed for the preparation of the nonimprinted butanethiol monolayer film but without the DNT (template).

Characterization of a 2-D Self-Assembled Butanethiol MIM. Resulting 2-D MIM and NIM were characterized with the aid of the following techniques: Ellipsometry was used to measure the thickness of the 2-D MIM and NIM film using a Multiskop ellipsometer (Optrel GmbH, Germany) equipped with a 632.8 nm laser. Contact angle measurements were performed on a CAM 200 optical contact angle meter (KSV Instruments Ltd.). Polarization modulation infrared reflection spectroscopy (PM-IRRAS) measurements were conducted using a Nicolet MAGNA-IR 860 Fourier transform spectrometer equipped with a liquid-nitrogen-cooled mercury−cadmium−telluride (MCT) detector and a Hinds Instruments PEM-90 photoelastic modulator operating at 37 kHz. X-ray photoelectron spectroscopy (XPS) measurements were made on a PHI 5700 X-ray photoelectron spectrometer. A research quartz crystal microbalance or RQCM obtained from MAXTEK, Inc. (now Inficon Corp.) was used for the QCM sensing experiments, and electrochemical impedance spectroscopy (EIS) analyses were performed on an Autolab general purpose electrochemical system (GPES) PGSTAT12 module equipped with a three-electrode cell and with a frequency response analyzer module (FRA). The Fit and Simulation version (v. 1.7) accompanying the FRA software allowed fitting of the circuit parameters to the measured data using the nonlinear least-squares method.

Detailed descriptions of the instrumentation specifications and procedures adopted in this study can be found in the Supporting Information.

Table 1. Calculated Stabilization Energies for the Complexes Formed between Different Alkylthiols of Varying Carbon Lengths and 2,4-Dinitrotoluene (DNT) Using Semiempirical PM3 Calculations (Spartan 08, Wavefunction Inc.)[a]

DNT−alkanethiol complexes	ΔE, kJ/mol	alkanethiol systems only	ΔE, kJ/mol
DNT and propanethiol	0.022	propanethiol	−409.84
DNT and butanethiol	−20.99	butanethiol	−526.29
DNT and dodecanethiol	−0.923	dodecanethiol	−1696.03
DNT and hexadecanethiol	28.873	hexadecanethiol	−2297.17
DNT and octadecanethiol	−6.6	octadecanethiol	−2571.13

[a] ΔH_f DNT = 109.61 kJ/mol.

RESULTS AND DISCUSSION

Theoretical Modeling of the Template−Alkylthiol Complex. Before considering the alkylthiol-based 2-D MIM as a recognition element for DNT, a theoretical study was performed by employing equilibrium geometry calculations in the ground state using the semiempirical method. PM3 was carried out using Spartan 08 (Wave function, Inc.) on the basis of the neglect of the diatomic differential overlap integral approximation. Semiempirical modeling is a key component in this study because it enables a better understanding of the molecular mode of interaction and subsequent binding of the complex adsorbate. Previous studies on SAM-based sensors have already utilized alkylthiols of varying chain lengths as recognition elements for sensor devices.[16−20] In an effort to select which among the *n*-alkylthiols would give a more favorable interaction with DNT, calculations were first performed on complexation with the following *n*-alkylthiols: *n*-propanethiol, *n*-butanethiol, dodecanethiol, hexadecanethiol, and octadecanethiol. The net stabilization energies calculated for alkanethiol and alkanethiol/DNT complex systems were obtained and are summarized in Table 1. The interaction energy between each alkanethiol and DNT was obtained from the calculated heats of formation using eq 1:

$$\Delta E = E_{2,\text{4-DNT - alkanethiol complex}} - [E_{\text{alkanethiol}} + E_{\text{DNT}}] \quad (1)$$

A negative value for ΔE denotes a favorable interaction between the monomer and the target analyte.[23]

It can be observed from Table 1 that among the alkanethiols modeled, butanethiol yielded the most stable complex with 2,4-DNT as suggested by the smallest ΔE. The calculated interaction energy for the butanethiol/DNT complex is −20.99 kJ/mol.

dx.doi.org/10.1021/la105128q |*Langmuir* XXXX, XXX, 000–000

On the basis of the orientation/conformation of each alkylthiol (energy minimized), it is assumed that the stability of the SAM is directly influenced by the ability of the monolayer to accommodate the template. Octadecanethiol exhibited the most highly ordered surface feature. Such a highly ordered structure actually serves as a barrier that prevents the migration of DNT within each alkyl chain. Thus, it may be inferred that a thiol monolayer formed with a longer alkyl chain will result in a film with a higher packing density, thereby hindering the formation of sites for possible binding of the DNT in a coadsorption process. In contrast, the flexibility of a shorter butyl chain may provide the necessary conformation for complex coadsorption (Figures 1 and S1, Supporting Information). Switching in SAMs, as termed by Weiss,[24] occurs when there is a change in hybridization at the molecule−substrate interface that goes with a change in the tilt of the adsorbate. Such chain dynamics observed for butanethiol may also be assumed to benefit from alkyl-phenyl interactions[25] that can exist between the methylene and methyl moieties of the alkyl chain and the phenyl of the DNT template. Also, as has been reported by Masunaga et al.,[26] shorter alkyl chains are favorable to the development of benzene-patterned SAMs. Thiol molecules containing longer alkyl chains tend to aggregate with each other rigidly, and defects that have a size and shape similar to those of benzene may not be maintained by these long-chain alkyl thiol molecules. This explains the observed stability of the butanethiol−DNT complex compared with that of complexes formed by other alkyl thiol systems.

Another interesting observation from the theoretical calculations is the relative stability of the octadecanethiol monolayer toward DNT compared with that of the hexadecanethiol monolayer. We ascribed this observation to the poor solubility of octadecanethiol in ethanol, which was used as a solvent to deposit the 2-D MIM. The solvation energy of ethanol may have moderated the dispersive forces in the octadecanethiol monolayer,[27] resulting in the deposition of a not so well ordered octadecanethiol monolayer on the gold surface. In effect, only a minimal energy barrier for electron transfer can be afforded by the octadecanethiol monolayer, suggesting the probable contribution of small defects to the integrity of the monolayer. This may have allowed template molecules to insert within these defects and contribute to the formation of the desired binding cavities within the monolayer.[28] Moreover, van der Waals interactions are more pronounced with the hexadecanethiol than with the octadecanethiol monolayer as implied by a more compact structure (i.e., the inter alkyl chain distances in hexadecanethiol monolayer were shorter than in the octadecanethiol system). As a result, some template molecules may have not managed to penetrate some portion of the hexadecanethiol monolayer surface, thereby hindering the formation of binding sites for the DNT.

Two-Dimensional Surface Imprinting by Solution Immersion of QCM Crystals in an Ethanol Solution of Alkylthiols. Butanethiol was thus chosen as the receptor on the basis of noncovalent interactions (weak attractive alkyl-phenyl interactions, van der Waals, etc.) that can exist between the methylene and methyl moieties of the alkyl chain and the phenyl groups of DNT. Butanethiol and DNT were then coadsorbed directly on the gold surface of a quartz crystal for subsequent QCM sensing. QCM permits in situ monitoring of the binding of DNT on a modified Au quartz crystal electrode surface. The imprinted monolayer film is interfaced with a piezoelectric transducer surface, enabling the determination of the binding kinetics. The changes in frequency of the quartz crystal can then be translated into the corresponding deposited mass on the surface through the Sauerbrey equation,[29]

$$\Delta f = -\frac{2{f_0}^2 \Delta m}{A(\rho_q \mu_q)^{1/2}} \quad (2)$$

where f_0 is the fundamental resonance frequency of the QCM (5 MHz), A is the area of the electrode (1.327 cm^2), ρ_q is the density of the quartz (2.65 g/cm^3), and μ_q is the shear modulus of the quartz (2.95×10^6 N/cm^2). The negative sign in the equation signifies that the adsorption of the analyte (DNT) on the 2-D MIM modified gold surface will result in a corresponding decrease in the frequency of the crystal (Figure S2, Supporting Information.[30]

From the theoretical modeling studies, a distinct surface structure is brought about by the coadsorption of the complex on the gold surface, enabling a more directed means of distributing the butanethiol on the gold surface to form pockets for DNT binding (Figure S3, Supporting Information). Most likely, the DNT−solvent complexes could have favorably occupied the pits/defects in the gold layer within the monolayer film,[31] interrupting the weak van der Waals interactions between the alkyl chains. This is not unreasonable because the probability of occupying the defect sites is higher as a result of the decreased packing density of the butanethiol molecules in these sites. Moreover, this increase in the degree of order of deposition on the surface of the matrix[32] has been shown to affect the rate of switching[33] of the adsorbate molecules as well as those of the inserted complexes (DNT−ethanol complex).[34] It has also been previously reported that the chemisorption efficiency depends on both the structural properties of the corresponding substrate constituent and the solvent used during the self-assembly process.[35] Stranick et al.[36] described the possible mechanism for the motion of the adsorbate molecules, which explains that the inserted rigid aromatic molecules may possibly move reversibly between the top and bottom of the step edge of the substrate. Thus, we assumed that this is also the case with a more favorable insertion of these DNT−ethanol complexes on the gold surface defect sites. It has been documented that benzene forms well-defined electronic interactions with metal surfaces.[37,38] Although the benzene−gold bond strength is relatively weak,[39] this allows DNT−ethanol complexation through H bonding to play a significant role. The phenyl ring of DNT can perturb the electronic structure of the gold surface, leading to a favorable adsorption of butanethiol followed by the DNT−ethanol complexes for the creation of binding pockets for DNT.

Nonetheless, it must be emphasized that different alkylthiols will have different binding affinities with different templates or analyte species.[14] In contrast to barbituric acid, DNT possesses an aromatic moiety that could have induced nonspecific interactions with the gold surface as well.[20,24,40] It has been found that the plane of such molecules can lie parallel to the substrate surface and that the interaction with the polar surface occurs predominantly through the π molecular orbitals of the DNT.[41,42] Though the benzene−gold bond strength is relatively weak,[39] these aromatic moieties may still cause perturbations to the electronic structure of the surrounding surface, leading to favorable sites for the coadsorption of DNT−ethanol complexes on the butanethiol SAM surface.

dx.doi.org/10.1021/la105128q |*Langmuir* XXXX, XXX, 000–000

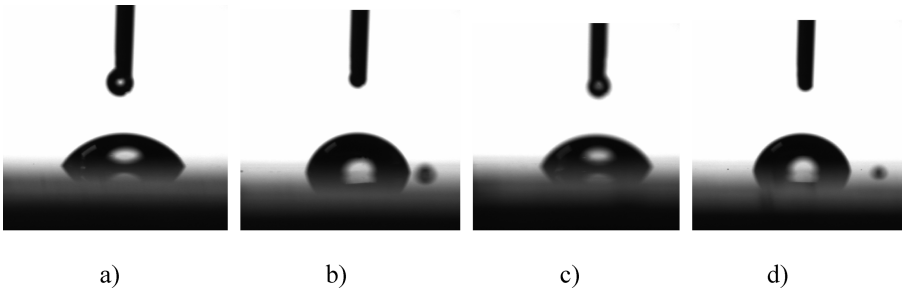

Figure 2. Captured images of the water contact angle formed on the surface of (a) a bare BK7 gold slide; (b) a DNT-imprinted butanethiol layer before template removal; (c) a DNT-imprinted butanethiol (NIM) layer after template removal; and (d) a nonimprinted butanethiol layer.

Optimization of Two-Dimensional MIM/QCM Surface Imprinting. The in situ QCM method is a convenient technique for monitoring the deposition of alkylthiol SAMs directly on the electrode surface. For sensing applications, optimizing the film/transducer interface requires a large surface/volume ratio advantage that is capable of providing fast rebinding kinetics[43] and should be robust and even reusable. Thus, to explore further the potential and utility of in situ QCM monitoring, QCM was used to optimize the preparation of the DNT-selective butanethiol 2-D MIM from solution. In particular, the time of deposition of the butanethiol monolayers was also investigated. Though most of the studies that have been reported stated that a mere 2 h is already enough to form the self-assembled layers of thiol, the QCM response as shown in Figure S5 in the Supporting Information indicates that overnight immersion (i.e., 12 to 20 h) would be favorable as indicated by a relatively higher frequency change so as to stimulate the equilibration of the template molecules with the gold substrate.

It is also recognized that in the preparation of SAMs for molecular recognition, the concentration of the template would also influence the formation of highly reliable sites during rebinding. As previously explained by Chailapakul and Crooks,[44] the template component induces defect sites within the monolayer to allow for the penetration of the target molecules. In principle, the number of defect sites can be reproducibly varied by changing the relative concentrations of the template and the alkanethiol molecules. In this study, we have adopted the same concentration of the template that was reported as optimum by Piletsky et al.[18] (i.e., 1% w/v); however, instead of using a 100 μM thiol concentration, we used 5 mM concentration. As a consequence, the DNT/C_4SH ratio was reduced. The rationale is to form as much as possible a monolayer having a low defect density. The relatively high concentration used for the template molecule was assumed to be more than enough to keep the effective competition between the thiol molecule and DNT for surface adsorption. A lower concentration for the template may not induce the formation of cavities within the monolayer.

Additionally, the thickness and wetting properties are important with respect to the bulk liquid or subphase to which the analyte will diffuse to the surface and into the film. The results show that the deposition of a butanethiol monolayer gave a relatively thinner film at ~0.56 nm (n = 20) (Table S1, Supporting Information) and is relatively hydrophilic (water contact angle = 82 ± 6°), which should be good for wettability in an aqueous medium. This should lead to unhindered diffusion of the DNT into the monolayer system.

However, the measured thickness of the butanethiol NIM is only ~0.38 nm (n = 8). This suggests a possible difference in the orientation of the butanethiol molecules in the presence of DNT at the surface. Optimized geometries obtained for the long-chain alkylthiols show that they are oriented more vertically with the thiol headgroup attached to the gold surface and exposing the methyl group. As a result, the contact angles increase because the methyl end-groups are intrinsically less polar than the methylene groups (Figure 2).[21] These geometries would support the thicknesses measured for the imprinted alkylthiol monolayers containing longer alkyl chains (C_{12} to C_{18}) using ellipsometry (i.e., from 1.3 to 1.7 nm), which did not exhibit significant imprinting. One may look at the possibility that without the template molecule the butanethiol molecules lay more flat and isotropically oriented across the gold surface, thus increasing the number of methylene units exposed on the surface.

Data on the apparent wettability and film thickness of the alkanethiol monolayer (compared to calculated values) implies some systematic error for these different alkanethiol systems that is due to the substrate's roughness and the gold layer being not rigorously flat.[21] Nevertheless, the role of the substrate in the switching process and its influence on the degree of order in the matrix cannot be discounted.[45] The surface interaction would reconfigure as the alkythiols change their tilt angles or hybridization,[24] subsequently affecting the mode of insertion of the DNT from the solution. In monolayer systems, previous studies have found that mixed monolayer films can be fabricated in which one component will distribute randomly in a matrix of a second component,[46] segregate into domains,[47] or be displaced from the film into solution by the second component.[48] Thus, it is further assumed that in the imprinted butanethiol monolayer film formed by the coadsorption of butanethiol and DNT, the molecular ordering was accomplished to an extent that the template and solvent molecules were driven to occupy primarily the defect sites in the gold layer.[21]

X-ray Photoelectron Spectroscopy (XPS) Studies. Sagiv[49] first reported that monolayers of alkylsiloxanes could effectively readsorb molecules of approximately the same size and shape as the molecules used to induce perforations on the surface. Chailapakul et al.[44] rationalized that such a strategy for molecular recognition may be due to the influence of the template component inducing defect sites within the inert framework, permitting the penetration of target molecules. Therefore, it should be significant to quantitatively characterize the butanethiol monolayer film composition with DNT as the target molecule. XPS was used to approximate the packing densities of both the 2-D MIM and NIM films. This can be done by obtaining the S/Au peak area ratios. XPS spectra were obtained from the film samples deposited on gold-coated BK7 glass. As earlier rationalized, more butanethiol molecules were deposited on the

dx.doi.org/10.1021/la105128q |*Langmuir* XXXX, XXX, 000–000

gold surface in the absence of a competing molecule such as DNT. Hence, the calculated S/Au peak area ratio is higher for the NIM (i.e., 0.014 as compared to only a 0.007 S/Au ratio obtained with the imprinted MIM). Figure S7 shows the S 2p peak of the imprinted and nonimprinted monolayer. Another interesting observation is that the S/Au peak ratio did not deviate largely before and after template removal and during the rebinding of DNT as shown in Table S2 in the Supporting Information, indicating the relative stability of the 2-D MIM on the gold surface. We have also ascertained the surface mass density from QCM and/or the apparent surface coverage by EIS and angle-resolved XPS (data not shown) upon the binding of DNT molecules both with the imprinted and nonimprinted butanethiol monolayers. Results show that the imprinted butanethiol monolayer exhibited greater surface coverage/density than did the nonimprinted butanethiol monolayer brought about by the binding of DNT molecules on the imprinted butanethiol surface. However, the C/Au peak ratios indicate that the ratios changed as the imprinting went through each process such as the deposition of an imprinted monolayer, ethanol washing to effect the removal of DNT, and the rebinding of DNT to the monolayer surface as shown in Table S2 in the Supporting Information.

In summary, the differentiation of chain conformation, orientation, coverage, and packing in monolayer structures of MIM versus NIM have been performed through molecular modeling studies, ellipsometry, and XPS. The results of these studies have demonstrated clear differences between MIM and NIM films. Molecular modeling studies have shown that the calculated net stabilization energy is lowest for the imprinted butanethiol monolayer. The average thicknesses obtained by ellipsometry indicate differences in the coverage of butanethiol molecules across the gold surface in the presence of DNT. The diffusion of DNT into the monolayer network may be influenced by the size and the density of the defect sites, leading to an overall translational ordering of the butanethiol lattice.[50] A moderately higher packing density was obtained for the NIM film as suggested by the higher S/Au peak area ratio calculated from the XPS data. To confirm the orientation and conformational order, PM-IRRAS studies were also conducted.

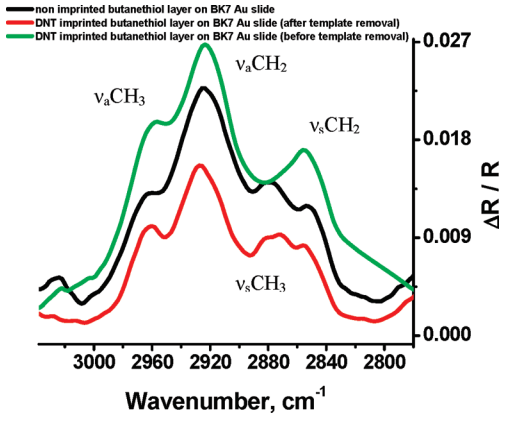

Figure 3. Plots of differential surface reflectivity, $\Delta R/R$, as a function of wavenumber for the different monolayer systems (i.e., nonimprinted and DNT imprinted before and after template removal). The differential surface reflectivity was calculated as $(R_p - R_s)/(R_p + R_s)$ where R_p and R_s represent the reflectivity for the respective polarization of light. The $\nu_a^{CH_2}$ peaks were reproducible to within ± 1 cm^{-1}.

Polarization Modulation Infrared Reflection Absorption Spectroscopy (PM-IRRAS) Studies. We stress the importance of the influence of the substructure of the MIM on the detection of DNT molecules, hence we considered the use of PM-IRRAS in characterizing the MIM and NIM monolayer structures on the gold substrate. The influence of the template molecules on the mode of deposition of MIM is clearly illustrated in this study. We ascertain that the conformational variations between MIM and NIM monolayer substructures may be attributed to the influence of the DNT molecules. It has been reported that benzene molecules are adsorbed to the gold surface via π-electron sharing.[51] 2,4-DNT, which contains an aromatic ring, poses a competition with the thiol molecules for adsorption sites on the gold surface. This consequently leads to the formation of defect sites whose size and shape complement those of the DNT template molecule. Such a structure construed high affinity sites for the rebinding of DNT molecules.

In particular, the 2-D orientation of the butanethiol molecules may be ascertained in the presence of the template DNT. As summarized in Figure 3 and Table 2, a comparison was made on the peak positions of the C−H stretching mode for the NIM and MIM before and after template removal. For a crystalline alkyl state, the following bands at 2918, 2851, and 2956 cm^{-1} pertain to asymmetric and symmetric CH_2 and CH_3 modes, respectively. Bands are shifted to higher wavenumbers for these C−H stretching modes (i.e., 2924, 2855, and 2957 cm^{-1} for a liquidlike state of thiol molecules).[52] Notably, the peak positions of the C−H stretching modes for both the MIM and NIM systems almost resemble those of the C−H stretching modes observed in a liquidlike state of alkylthiols. Hence, the average local environment for both monolayer systems is more similar to that of the liquid phase (i.e., isotropic and disordered). As a consequence, less densely packed monolayer structures were assumed to be deposited on the gold surface, resulting in a low surface coverage for both NIM and MIM. If this is the case, then inter- and

Table 2. Peak Positions for C−H Stretching Modes in an Imprinted and Nonimprinted Butanethiol Monolayer Adsorbed on a Gold Surface[a]

		peak positions for crystalline and liquid states, cm^{-1}		peak positions for butanethiol adsorbed on gold, cm^{-1}		
structural group	C−H stretching mode	crystalline	liquid	nonimprinted	imprinted before template removal	imprinted after template removal
$-CH_2-$	ν_a	2918	2924	2924	2923	2926
	ν_s	2851	2855	2852	2855	2855
CH_3-	ν_a	2956	2957	2961	2956	2960

[a] The $\nu_a^{CH_2}$ peaks were reproducible to within ± 1 cm^{-1}.

dx.doi.org/10.1021/la105128q |Langmuir XXXX, XXX, 000–000

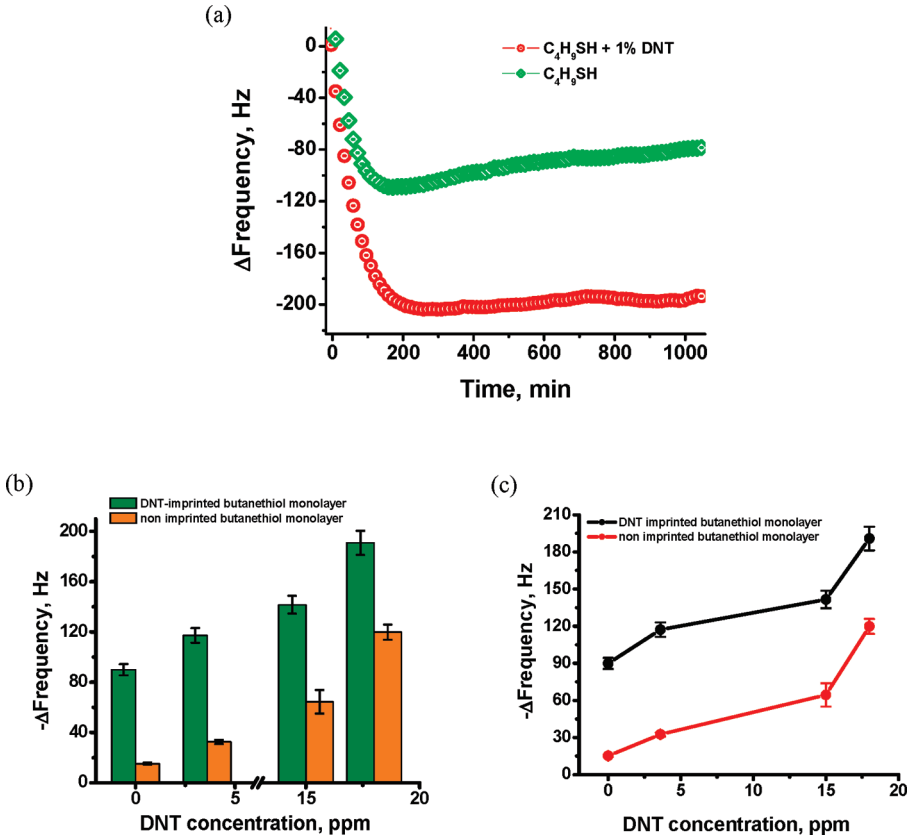

Figure 4. QCM responses of a DNT imprinted and nonimprinted butanethiol layer upon exposure to 18 ppm DNT in an acetonitrile/water 1:9 v/v solution (Figure S6, Supporting Information): (a) plot of the change in frequency as a function of time; (b) bar graph depicting the changes in frequency of the quartz crystal as a function of the increasing concentrations of DNT (note that the frequency shifts have a negative magnitude); (c) calibration plot showing the change in frequency as a function of DNT concentration in ppm.

intrachain interactions are minimized, which could result in some butanethiol molecules desorbing from the gold surface. This probably explains some of the nonspecific adsorption observed with selectivity experiments in which molecules of almost similar structures to DNT tend to be adsorbed on the surface of the MIM film (discussion in the succeeding section). It is possible that these analogues may have competed with butanethiol for binding sites on the gold surface, causing the desorption of some butanethiol molecules (as evidenced by QCM). This is in contrast to more crystalline or orthogonally oriented long-alkyl-chain SAMs used for MIM.[13]

Analytical Performance of the MIM/QCM Sensor. *Sensor's Response to Varying Concentrations of DNT.* Figure 4 gives the QCM response of the MIM film against the NIM butanethiol layer in sensing DNT. The MIM gave the most pronounced decrease in frequency, thus confirming successful imprinting. The frequency shift as a function of time (kinetics curve) of the QCM is also shown in Figure 4a. The correction of these frequency changes by a deduction of the frequency change recorded for the binding of DNT with the nonimprinted monolayer with respect to the frequency change noted for the rebinding of DNT with the imprinted monolayer showed an average frequency shift of -76.9 ± -5.8 Hz that was due to the actual binding of DNT. Correction is necessary so as to account for the surface roughness of the gold substrate and the presence of some physisorbed molecules on the gold surface.[53]

The MIM film was exposed to varying concentrations of DNT (i.e., 0, 20, 80, and 100 μM). These roughly correspond to 0−18 ppm DNT concentration range. A calibration curve was obtained from the plot of the change in frequency as a function of DNT concentration as shown in Figure 4b,c. A linear response was obtained within this concentration range of DNT with $R^2 = 0.950$.

Recognition Selectivity of the DNT-Imprinted MIM. The selectivity figure of merit of the DNT 2-D MIM was investigated by exposing the monolayer film to 18 ppm solutions of 2,4-dinitrophenol, 2, 6-dinitrotoluene, 4-nitrotoluene, and toluene (data not shown here). The structures of these compounds are similarly related to that of DNT. The bar chart, shown in Figure 5, indicates the changes in frequency upon exposure of the MIM film in each solution of the competing molecule. Unlike studies conducted by Piletsky et al.[18] and Bi and Yang,[22] the selectivity of the imprinted hexadecylmercaptan and octanethiol monolayers toward cholesterol, thiachloprid, and imidacloprid, respectively, was not demonstrated. Although the MIM butanethiol layer exhibited selectivity toward DNT, it also accommodated toluene. The binding of toluene and 4-nitrotoluene may be due to the small size of these molecules relative to DNT. Because the cavities formed within the MIM were larger, these molecules could easily fit in and get trapped within the porous network during exposure. For 2,4-dinitrophenol, steric crowding and H-bonding may be factors aside from the fact that its size and shape does not exactly fit the size and shape of the DNT template

dx.doi.org/10.1021/la105128q |*Langmuir* XXXX, XXX, 000–000

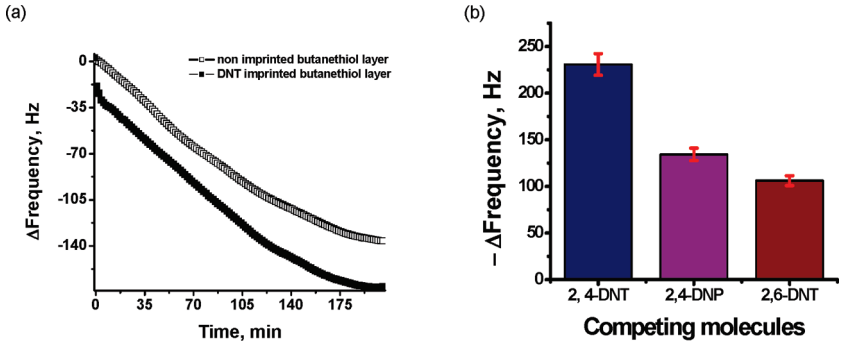

Figure 5. (a) Observed changes in frequency of the QCM crystal (5 MHz) upon the rebinding of competing molecules to both imprinted (MIM) and nonimprinted monolayer (NIM) films demonstrating the relative sensitivity of the imprinted monolayer film toward DNT in a mixture of 2,4-DNT, 2,4-DNP, 2,6-DNT, toluene, and 4-nitrotoluene. (b) Bar graph showing the relative selectivity of the monolayer film when individually exposed to each of the competing molecules. (Data for toluene and 4-nitrotoluene are not shown.)

because of the presence of a more electronegative atom (−OH vs $-CH_3$). Therefore, it is presumed that aside from the requirement that the size and shape of the binding sites must be complementary with the template, contributions of nonspecific hydrophobic interactions to the strength of monolayer−template interactions may also be in effect and significant in an aqueous medium. Karlsson et al.[54] have demonstrated that the mechanistic basis for recognition was entropy-driven in aqueous media, wherein nonspecific hydrophobic interactions are strong.

What is interesting in this experiment, though, is that the MIM was capable of differentiating 2,4-DNT and 2,6-DNT as demonstrated by the moderately large difference in the frequency shift of the 2-D MIM/QCM sensor. The larger shift in the frequency for 2,4-DNT still indicates that more of these molecules were bound to the 2-D MIM/QCM sensor film.

To quantify the observations further, data obtained from the original plot (Figure S9, Supporting Information) were used to calculate for the % cross selectivity[55] of the 2-D MIM/QCM film sensor. The efficiency of DNT binding to the imprinted cavities is best described by the cross selectivity ratio (CSR). The CSR is referred to as the ratio of the change in frequency observed upon binding of the competing molecule to the change in frequency when the film was exposed to a solution containing the target analyte (i.e., $\Delta f_{x\ \mathrm{molecule}}/\Delta f_{\mathrm{DNT}}$). The relative cross selectivity of the imprinted 2,4-DNT against the three molecules follows this trend: toluene (= 84.6%) > 4-nitrotoluene (= 73.1%) > 2,4-dinitrophenol (= 57.7%) > 2,6-dinitrotoluene (= 48.1%). A small CSR indicates very little and/or the absence of interaction between the imprinted polymer film and a competing molecule. A large value indicates strong competition in mixed solutions of the analyte and the other molecule. Although the results show that the 2-D MIM of butanethiol exhibited poor selectivity when exposed to molecules with a similar shape that were equal to or smaller in size than the original template, they are able to demonstrate good selectivity with other isomers of the analyte. This feature may be of importance because most 3D MIPs have poor selectivity with close configurational and structural isomers of the original template.[56] It is also worth noting that the MIM film demonstrated sensitivity toward DNT even in a mixed solution of DNT, 2,4-dinitrophenol, toluene, and 4-nitrotoluene. Even though the QCM may not be the best technique to differentiate among the molecules or bind strongly with the monolayer (compared to SPR, ellipsometry, waveguiding, etc.), still it was able to demonstrate that the MIM gave a more significant change in frequency as opposed to the NIM film (Figure 5a), which may suggest practical applications in the preparation of a cross-reactive sensor array.

Nonspecific binding is a common observation to studies employing the concept of self-assembled monolayers. Though self-assembled MIM provides a simple and robust means of modifying sensor surfaces, the degree of selectivity for these types of sensors seems to be limited, as mentioned by Li and Husson.[21] However, in this study we were able to demonstrate a good compromise among sensitivity, selectivity, and robustness toward nitroaromatic compounds. The 2-D MIM/EIS sensor can discriminate DNT from other competing nitroaromatic compounds, and its selectivity was found to vary from one molecule to another. To this end, we generalized that 2-D alkylthiol-based MIM may have different capacities (hydrophobic, hydrogen bonding, weak van der Waals interactions, etc.) toward the analyte, which may or may not result in the detection of the target compounds. This suggests promising applications in field detection of nitroaromatic compounds. Several papers have reported the use of semiselective[57] sensors for the detection of nitroaromatic compounds, but other sensor types are designed to be nonspecific and cross reactive.[58]

The selectivity test conducted using the butanethiol MIM demonstrates its ability to readsorb the original templated molecule, and therefore highlights its use as a sensor for DNT with some limitations. However, it is further noted that the imprinted alkylthiol monolayer manifested different capacities because of the nature of its interactions with the template. As in the other cases of molecular imprinting, this capacity of 2-D MIM may or may not facilitate the detection of DNT and other nitroaromatic compounds. On the basis of these results, it should be possible to demonstrate this concept with 2,4,6-trinitrotoluene (TNT) under appropriate and safe protocols.

Sensing via Electrochemical Impedance Spectroscopy. EIS was used to corroborate the QCM data in which both MIM and NIM films were exposed to various concentrations of DNT. The technique is useful for examining in detail the physical factors controlling the analytical sensitivity and interfacial properties of films deposited on the gold substrate as the analyte binds to it. The SAMs deposited on the electrode surface obstruct the approach of the electron to the electrode surface. This reduces the electrical capacitance of the SAM electrode and increases the resistance of the electrode. Although several studies on biosensing, particularly protein binding, have employed EIS for signal

dx.doi.org/10.1021/la105128q |*Langmuir* XXXX, XXX, 000–000

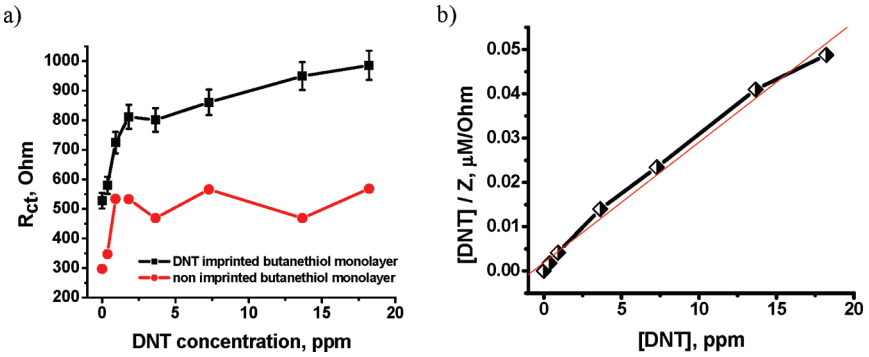

Figure 6. (a) Variation of R_{ct} upon binding of DNT molecules with the imprinted and nonimprinted butanethiol monolayer systems. (b) Dependence of the total impedance on increasing DNT concentrations: calibration plot of the DNT sensor.

transduction,[59] Chailapakul and Crooks[44] reported the permeability of a long-chain alkanethiol for two electroactive probes: $Ru(NH_3)_6^{3+}$ and $Fe(CN)_6^{3-}$. However, they did not show the influence of the template or the effect of structurally similar molecules on this process. In this study, EIS was used as an ex situ or indirect detection technique to monitor DNT binding with the MIM and NIM films prepared on gold-coated BK7 glass slides. Briefly, the binding of the DNT molecules on the 2-D monolayer film caused the decrease in the electrochemical current brought about by an impediment in the flow of the electrons in an ac circuit. DNT molecules blocked the electrode surface, and the extent of such blockage is dependent on the concentration of DNT.[60] Changes in total impedance obtained during the rebinding of the different concentrations of DNT on the imprinted 2-D MIM were used to calculate the amount of DNT using the equation of the line, $Z = 8.6[\mathrm{DNT}] + 1219.3$ ($R^2 = 0.977$). The sensitivity of the sensor, which is a measure of its ability to discriminate between small differences in DNT concentration, was found to be equal to 8.6 Ω/μM (5.1 Ω/ppm). The detection limit, which gives the minimum concentration of DNT that can be detected at a known confidence level, was calculated to be 41.9 μM (or approximately 7.6 ppm).

In fitting the EIS data, the Randles circuit represented by $R_s(C1[R_{ct}W])$ was adopted to model the rebinding of DNT with the MIM. This equivalent circuit is preferentially used to model modified surfaces with defects/channels for ion transport or adsorption. $C1$ pertains to the capacitance of the film, R_{ct} is the charge-transfer resistance, R_s is the resistance of the electrolyte solution and reference electrode, and W refers to the Warburg resistance. This model represents the physical structure of the interface in terms of three layers, each with its own unique electrical properties: (1) electrolyte; (2) molecular layer, which represents the MIM or NIM; and (3) the gold substrate as illustrated in Figure S10, Supporting Information.

For EIS indirect sensing, a 5 mM $K_3Fe(CN)_6$ probe was used to obtain quantifiable impedance spectra and minimize the "repeated measurement-related" R_{ct} increase. An experiment using NIM was also performed to validate the assumption that changes in the charge-transfer resistance were due to the binding of DNT to the butanethiol monolayer. Results show that the binding of DNT to butanethiol-modified gold surfaces is governed by resistance in the molecular layer (charge-transfer resistance) and takes place at low frequencies. As shown in Figure 7, the radius of the semicircle in the Nyquist plot of the MIM is much larger than that observed in the NIM film. This indicates the preferential and specific association of DNT to the

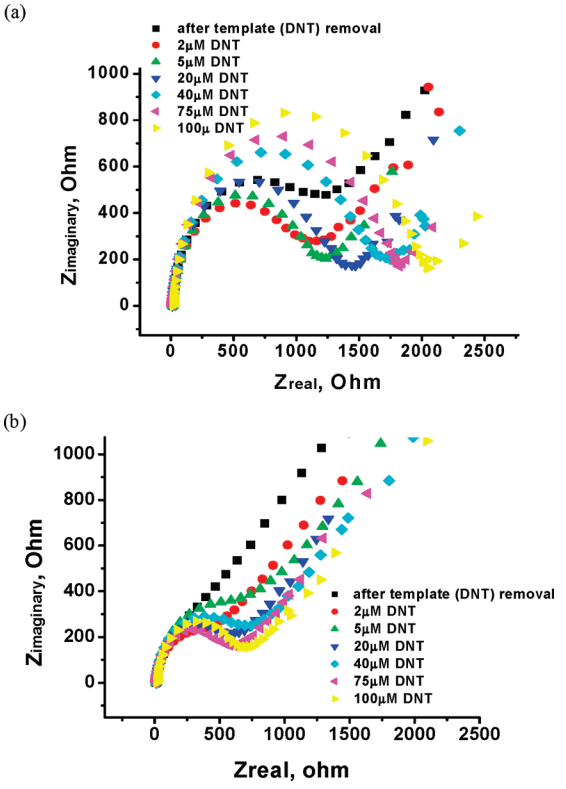

Figure 7. Faradaic impedance spectra obtained in 0.5 M sodium sulfate containing 5 mM $K_3Fe(CN)_6$ at the monolayer modified gold surface: (a) imprinted (MIM) and (b) nonimprinted (NIM, control) in the absence and presence of DNT.

imprinted monolayer network. Such an increase in the charge-transfer resistance may also be due to the electrostatic repulsion in the presence of the NO_2 groups of DNT with the negatively charged $Fe(CN)_6^{3-/4-}$. Moreover, the noted increase in the radius of the semicircle is a function of the concentration of DNT as shown in Figure 7.

Figure 7 gives the variation of the total impedance as a function of increasing concentrations of DNT. As shown in Figure 7a, the impedance decreases from 550 to 400 Ω upon the binding of DNT molecules. Accordingly, the charge-transfer resistance, R_{ct} initially decreases (against the charge-transfer resistance of MIM after template removal) upon the binding of DNT with the imprinted butanethiol monolayer but continues to change as the

dx.doi.org/10.1021/la105128q |*Langmuir* XXXX, XXX, 000–000

DNT concentration is increased. Simply, this goes to show that some surface effects and DNT binding on the imprinted butanethiol monolayer may experience a degree of conformational effects (surface reorganization)[61] or swelling[62] that requires further experimental proof. However, the electron-transfer resistance obtained from the binding of DNT molecules with the nonimprinted butanethiol monolayer implies that the sensing layer or the probe is sufficiently small to penetrate freely through these pinholes, and therefore displays a moderate and similar affinity to varying concentrations of DNT.[63] Moreover, the observed overlap of the traces for the binding of DNT with the nonimprinted butanethiol monolayer illustrates the possible saturation of the surface, and the impedance shows either very little or no further change.

The experimental values obtained in this study were also used to establish the relationship of the impedance with DNT concentration in the bulk. This can be done by employing the Langmuir adsorption isotherm, which assumes monolayer adsorption. The Langmuir equation adopted for this study, as also reported by Fragoso et al.,[64] is expressed as

$$\frac{c}{Z_{max}} + \frac{1}{K_a Z_{max}} = \frac{c}{Z} \quad (5)$$

where c/Z is the impedance at a given concentration and K_a gives the equilibrium (association) constant, Z_{max} is the saturation impedance, and c is the concentration of DNT. Upon fitting of the experimental data, the binding kinetics of DNT to the 2-D butanethiol monolayer is shown to fit the Langmuir model. This suggests that the binding of DNT to the 2-D monolayer film involves the monolayer adsorption of DNT molecules. Fitting of the experimental data gives the equation $c/Z = 4.95 \times 10^{-4}$ [DNT] + 0.0019, ($R^2 = 0.9949$). From this equation, the experimental K_a is obtained to be 1.1×10^6 μM/Ω. The association constant reflects the changes in the enthalpy associated with the interaction of the imprinted butanethiol monolayer with DNT molecules, which may be due to the following factors: differences in the solvation of the rebinding medium, $\pi-\pi$ stacking of DNT molecules, steric deformation brought about by the rebinding of DNT molecules, and intra- and interalkyl chain interactions.[65] Specifically, the association constant obtained from EIS sensing manifests the interaction of the DNT molecules with the imprinted butanethiol monolayer surface. The value shows the ratio of the change in DNT concentration with the total impedance.

Although the values shown above are the calculated values obtained with 2-D MIM/EIS, the experimentally determined relative sensitivity of the 2-D MIM/QCM technique toward DNT molecules was separately established to be 0.80 Hz/μM (5.6 Hz/ppm) and the detection limit was 29.5 μM (5.4 ppm). A moderately lower detection limit was obtained with the QCM as a transducer. Nevertheless, both techniques have been demonstrated to be capable of quantifying the number of DNT molecules that bind with the 2-D MIM film, and the two techniques exhibit robustness in the sense that they can easily be interfaced with a flat electrode transducer for sensing applications. It is acknowledged that the calculated detection limits obtained in this study are significantly higher than the detection limits of explosives using conjugated polymer-based sensors. Zeller et al.[66] have emphasized that the need for a properly calibrated sensor may not be necessary for field use as long as the sensor has a defined limit of recognition for its intended target species because of the varying levels of DNT in the environment. Albert and Walt[67] have also expressed the same explanation that if a sensor has the ability to recognize DNT regardless of concentration levels or background interferences it might be useful for land mine detection. Moreover, although QCM permits the investigation of the viscoelastic behavior of the 2-D butanethiol monolayer films upon interaction with DNT (Figure S4, Supporting Information), the EIS technique proves to be important in characterizing the electrochemical properties at the gold−butanethiol interface as DNT binds with the monolayer film. Thus, both techniques were able to provide useful information related to the changes on the monolayer surface upon the rebinding of the template molecule (DNT).

In summary, EIS has been shown to be a useful technique for investigating and evaluating DNT sensing with the 2-D MIM films. Differences in the surface properties of bare gold, MIM, and NIM films have been clearly illustrated. Such differences may be attributed to the presence of holes/defects that were formed on the monolayer surface with the imprinting of DNT, a nitroaromatic compound. Though the EIS results imply variation in the capacitance dispersion of both MIM and NIM compared with bare gold, it was also demonstrated that these variations on the substructure of the MIM and NIM may be attributed to the microscopic roughness of the electrode,[68] the presence of inhomogeneities at the electrode surface on the atomic scale,[69] and the specific sorption of molecules on the electrode surface.[70] It was shown that the NIM film exhibited good insulating properties and significant capacitive behavior. However, Warburg impedance was more pronounced with the MIM film as the phase angle shifted to approximately 45°. The binding trend of DNT to the MIM film was studied with a redox probe, $K_3Fe(CN)_6$. It was shown that the radius of the semicircle, which represents the charge-transfer phenomenon, tends to increase with increasing concentrations of the incorporated DNT. Moreover, the radius observed for the binding of DNT with the MIM was found to be relatively large compared to that of the NIM film.

CONCLUSIONS

A sensor was prepared from SAMs of butanethiol on a gold surface or 2-D MIMs using 2,4-DNT as a model nitroaromatic compound. The self-assembly technique offers the advantage of simplicity in the preparation of a sensor for nitroaromatic compounds. The challenge of preparing a MIM-based sensor lies on the choice of the right alkylthiol. For instance, the use of the shorter butane thiol together with the DNT template was justified. Contributions of chain conformation, orientation, coverage, and packing to changes in monolayer structures of the MIM and NIM films were confirmed through molecular modeling studies, ellipsometry, XPS, SPR, and PM-IRRAS. It may be summarized that the structural properties of alkylthiol-based MIMs are influenced by (a) intra- and intermolecular interactions and (b) commensurate arrangement of cross-sectional areas of molecular components in 2-D. Molecular modeling studies have been shown to be useful for calculating the net stabilization energies, guiding the use of a particular alkylthiol−template combination. Ellipsometry, XPS, SPR, and PM-IRRAS measurements confirmed differences in the coverage of butanethiol molecules across the gold surface on the MIM and NIM films as influenced by the size and density of the defect sites. A switching mechanism was invoked to confirm the overall translational ordering of the butanethiol lattice with and without the DNT template. QCM

dx.doi.org/10.1021/la105128q |*Langmuir* XXXX, XXX, 000–000

was used as a signal transducer to monitor the binding and sensing of various concentrations of DNT and competing analogs. Calibration plots obtained from QCM responses as a function of the concentration of the template showed a linear response. Also, DNT exhibited selectivity in the presence of structurally similar molecules but showed poorer selectivity compared to smaller analogues. Functionalizing the butanethiol end-group with a cross-linkable or reactive end-group may be explored in the future in order to address the stability issues after template removal. Moreover, studies on crystalline or terraced Au(111) may enable more insight into the role of the Au substrate in facilitating the suggested switching mechanism for template insertion and defect site cavitation preference in MIMs.

This study also emphasized the use of EIS to monitor the binding of DNT with the MIM film. The EIS technique has been a popular transduction system for biosensing, in particular, for those involving protein binding. Thus, future EIS sensing using the 2-D MIM method may be applicable to larger biomolecules. EIS was shown to be effective in describing the interfacial properties of the films. Aside from this capability, EIS can also be used as a signal transducer for DNT, confirming the results obtained by QCM. Future studies will be undertaken for further optimization of this proposed detection scheme for DNT and other nitroaromatic compounds. Additionally, it is worth exploring to employ this molecularly imprinted alkyl monolayer (MIM) for the fabrication of a cross-reactive sensor array in the detection of nitroaromatic compounds.

■ ASSOCIATED CONTENT

Supporting Information. QCM kinetics measurements, molecular models, thickness data, and so forth. This material is available free of charge via the Internet at http://pubs.acs.org.

■ AUTHOR INFORMATION

Corresponding Author

*E-mail: radvincula@uh.edu. Phone: +1 713 743 1755.

■ ACKNOWLEDGMENT

We acknowledge funding from the National Science Foundation CBET-0854979, DMR-10-06776, and Robert A. Welch Foundation E-1551. D.C.A. We acknowledge funding from the Department of Science and Technology (DOST), Philippine Government, the Philippine Council for Advanced Science and Technology Research Development (PCASTRD) and Mines and Geosciences Bureau-Department of Environment and Natural Resources (MGB-DENR). We also acknowledge technical support from Inficon Inc., Agilent Technologies, and Chris Jameson for his help with the PM-IRRAS analysis.

■ REFERENCES

(1) Walker, N. R.; Linman, M. J.; Timmers, M. M.; Dean, S. L.; Burkett, C. M.; Lloyd, J. A.; Keelor, J. D.; Baughman, B. M.; Edmiston, P. L. *Anal. Chim. Acta* **2007**, *593*, 82.

(2) Jose, A.; Zhu, Z.; Madigan, C. F.; Swager, T. M.; Bulovic, V. *Nature* **2005**, *434*, 876.

(3) MacQuade, D. T.; Pullen, A. E.; Swager, T. M. *Chem. Rev.* **2000**, *100*, 2537.

(4) Albert, K. J.; Lewis, N. S.; Schauer, C. L.; Sotzing, G. A.; Stitzel, S. E.; Vaid, T. P.; Walt, D. R. *Chem. Rev.* **2000**, *100*, 2595.

(5) Lehn, J. M. *Angew. Chem., Int. Ed.* **1990**, *29*, 1304.

(6) Harrison, K.; Kang, J. F.; Haasch, R. T.; Kilbey, S. M., II *Langmuir* **2001**, *17*, 6560.

(7) Dubois, L. H.; Nuzzo, R. G. *Annu. Rev. Chem.* **1992**, *43*, 437.

(8) Kim, H. I.; Graupe, M.; Oloba, O.; Koini, T.; Immaduddin, S.; Lee, T. R.; Perry, S. S. *Langmuir* **1999**, *15*, 3179.

(9) Quon, R. A.; Ulman, A.; Vanderlick, T. K. *Langmuir* **2000**, *16*, 3797.

(10) Huan, S.; Hu, S.; Shen, G.; Yu, R. *Anal. Lett.* **2003**, *36*, 2401.

(11) Colorado, R.Lee, T. R. In *Encyclopedia of Materials: Science and Technology*; Buschow, K. H. J., Cahn, R. W., Flemings, M. C., Ilschner, B., Kramer, E. J., Mahajan, S., Eds.; Elsevier: Oxford, U.K., 2001; p 9332

(12) (a) Nuzzo, R. G.; Allara, D. L. *J. Am. Chem. Soc.* **1983**, *105*, 4451. (b) Laibinis, P. E.; Fox, M. A.; Folkers, J. P.; Whitesides, G. M. *Langmuir* **1991**, *7*, 3167.

(13) Ulman, A. *Chem. Rev.* **1996**, *96*, 1533.

(14) Blanco-Lopez, M. C.; Lobo-Castanon, M. J.; Miranda-Ordieres, A. J.; Tunon-Blanco, P. *Trends Anal. Chem.* **2004**, *23*, 36.

(15) (a) Sagiv, J. *Isr. J. Chem.* **1979**, *18*, 346. (b) Chidsey, C. E. D.; Bertozzi, C. R.; Putvinski, T. M.; Mujsce, A. M. *J. Am. Chem. Soc.* **1990**, *112*, 4301.

(16) Mirsky, V. M.; Riepl, M.; Wolfbeis, O. S. *Biosens. Bioelectron.* **1997**, *12*, 977.

(17) Lahav, M.; Katz, E.; Doron, A.; Patolsky, F.; Willner, I. *J. Am. Chem. Soc.* **1999**, *121*, 862.

(18) Piletsky, S. A.; Piletskaya, E. V.; Sergeyeva, T. A.; Panasyuk, T. L.; El'skaya, A. V. *Sens. Actuators, B* **1999**, *60*, 216.

(19) Chou, L. C. S.; Liu, C.-C. *Sens. Actuators, B* **2005**, *110*, 204.

(20) Mirsky, V. M.; Hirsch, T.; Piletsky, S. A.; Wolfbeis, O. S. *Angew. Chem., Int. Ed.* **1999**, *38*, 1108.

(21) Li, X.; Husson, S. M. *Langmuir* **2006**, *22*, 9658.

(22) Bi, X.; Yang, K.-L. *Anal. Chem.* **2009**, *81*, 527.

(23) (a) Holdsworth, C. I.; Bowyer, M. C.; Lennard, C.; McCluskey, A. *Aust. J. Chem.* **2005**, *58*, 315. (b) Schwarz, L.; Bowyer, M. C.; Holdsworth, C. I.; McCluskey, A. *Aust. J. Chem.* **2006**, *59*, 129. (c) Schwarz, L.; Holdsworth, C. I.; McCluskey, A.; Bowyer, M. C. *Aust. J. Chem.* **2004**, *57*, 759.

(24) Weiss, P. S. *Acc. Chem. Res.* **2008**, *41*, 1772.

(25) Watson, A. E. P.; McLure, I. A.; Bennett, J. E.; Benson, G. C. *J. Phys. Chem.* **1965**, *69*, 2753.

(26) Masunaga, K; Michiwaki, S; Izumi, R.; Ivarsson, P; Bjorefors, F.; Lundstrom, I.; Hayashi, K.; Toko, K. *Sens. Actuators, B* **2008**, *130*, 330.

(27) Kim, D. H.; Noh, J.; Hara, M.; Lee, H. *Bull. Korean Chem. Soc.* **2001**, *22*, 276.

(28) Krysinski, P.; Moncelli, M. R.; Tadini-Buoninsegni, F. *Electrochim. Acta* **2000**, *45*, 1885.

(29) Sauerbrey, G. *Z. Phys.* **1959**, *155*, 206.

(30) (a) Willicut, R. J.; McCarley, R. L. *Adv. Mater.* **1995**, *7*, 759. (b) Lukkari, J.; Alanko, M.; Pitkanen, V.; Kleemola, K.; Kankare, J. *J. Phys. Chem.* **1994**, *98*, 8525.

(31) Cygan, M. T.; Dunbar, T. D.; Arnold, J. J.; Bumm, L. A.; Shedlock, N. F.; Burgin, T. P.; Jone, L., II; Allara, D. L.; Tour, J. M.; Weiss, P. S. *J. Am. Chem. Soc.* **1998**, *120*, 2721.

(32) Donhauser, Z. J.; Mantooth, B. A.; Kelly, K. F.; Bumm, L. A.; Monnell, J. D.; Stapleton, J. J.; Price, D. W.; Rawlett, A. M.; Allara, D. L.; Tour, J. M.; Weiss, P. S. *Science* **2001**, *292*, 2303.

(33) Donhauser, Z. J.; Mantooth, B. A.; Pearl, T. P.; Kelly, K. F.; Nanayakkara, S. U.; Weiss, P. S. *Jpn. J. Appl. Phys.* **2002**, *41*, 4871.

(34) Moore, A. M.; Mantooth, B. A.; Donhauser, Z. J.; Maya, J.; Price, D. W., Jr.; Yao, Y.; Tour, J. M.; Weiss, P. S. *Nano Lett.* **2005**, *5*, 2292.

(35) Love, J. C.; Estoff, L. A.; Kriebel, J. K.; Nuzzo, R. G.; Whitesides, G. M. *Chem. Rev.* **2005**, *105*, 1103.

(36) Stranick, S. J.; Parikh, A. N.; Allara, D. L.; Weiss, P. S. *J. Phys. Chem.* **1994**, *98*, 11136.

(37) Munakata, T. *J. Chem. Phys.* **1999**, *110*, 2736.

(38) Munakata, T. *Surf. Sci.* **2000**, *454*, 118.

(39) Mantooth, B. A.; Sykes, E. C. H.; Han, P.; Moore, A. M.; Donhauser, Z. J.; Crespi, V. H.; Weiss, P. S. *J. Phys. Chem. C* **2007**, *111*, 6167.

(40) Clegg, R. S.; Hutchison, J. E. *Langmuir* **1996**, *12*, 5239.
(41) Koel, B. E.; Crowell, J. E.; Mate, C. M.; Somorjai, G. A. *J. Phys. Chem.* **1984**, *88*, 1988.
(42) Waddill, G. D.; Kesmodel, L. L. *Phys. Rev. B* **1985**, *31*, 4940.
(43) Riskin, M.; Tel-Vered, R.; Bourenko, T.; Granot, E.; Willner, I. *J. Am. Chem. Soc.* **2008**, *130*, 9726.
(44) Chailapakul, O.; Crooks, R. M. *Langmuir* **1993**, *9*, 884.
(45) Moore, A. M.; Mantooth, B. A.; Donhauser, Z. J.; Yao, Y.; Tour, J. M.; Weiss, P. S. *J. Am. Chem. Soc.* **2007**, *129*, 10352.
(46) Takami, T.; Delamarche, E.; Michel, B.; Gerber, Ch.; Wolf, H.; Ringsdorf, H. *Langmuir* **1995**, *11*, 3876.
(47) Stranick, S. J.; Parikh, A. N.; Tao, Y.-T.; Allara, D. L.; Weiss, P. S. *J. Phys. Chem.* **1994**, *98*, 7636.
(48) Folker, J. P.; Laibinis, P. E.; Whitesides, G. M.; Deutch, J. *J. Phys. Chem.* **1994**, *98*, 563.
(49) (a) Sagiv, J. *J. Am. Chem. Soc.* **1980**, *102*, 92. (b) Sagiv, J. *Isr. J. Chem.* **1979**, *18*, 339.
(50) Bain, C. D.; Troughton, E. B.; Tao, Y. T.; Evall, J.; Whitesides, G. M.; Nuzzo, R. G. *J. Am. Chem. Soc.* **1989**, *111*, 321.
(51) (a) Montilla, F.; Huerta, F.; Morrallon, E.; Vazquez, J. L. *Electrochim. Acta* **2000**, *45*, 4271. (b) Wetterer, S. M.; Lavrich, D. J.; Cummings, T.; Bernasek, S. L.; Scoles, G. *J. Phys. Chem. B* **1998**, *102*, 9266.
(52) Porter, M. D.; Bright, T. B.; Allara, D. L.; Chidsey, C. E. D. *J. Am. Chem. Soc.* **1987**, *109*, 3559.
(53) Kim, D. H.; Noh, J.; Hara, M.; Lee, H. *Bull. Korean Chem. Soc.* **2001**, *22*, 276.
(54) Karlsson, J. G.; Andersson, L. I.; Nicholls, I. A. *Anal. Chim. Acta* **2001**, *435*, 57.
(55) (a) Batra, D.; Shea, K. J. *Curr. Opin. Chem. Biol.* **2003**, *7*, 434. (b) Vlatakis, G.; Andersson, L. I.; Muller, R.; Mosbach, K. *Nature* **1993**, *361*, 645.
(56) (a) Fischer, L.; Muller, R.; Ekberg, B.; Mosbach, K. *J. Am. Chem. Soc.* **1991**, *113*, 9358. (b) Haginaka, J.; Sakai, Y.; Narimatsu, S. *Anal. Sci.* **1998**, *14*, 823.
(57) (a) Yang, J. S.; Swager, T. M. *J. Am. Chem. Soc.* **1998**, *120*, 5321. (b) Yang, J. S.; Swager, T. M. *J. Am. Chem. Soc.* **1998**, *120*, 11864. (c) Swager, T. M. *Acc. Chem. Res.* **1998**, *31*, 201–207.
(58) (a) Albert, K. J.; Walt, D. R. *Anal. Chem.* **2000**, *72*, 1947. (b) Dickinson, T. A.; Michael, K. M.; Kauer, J. S.; Walt, D. R. *Anal. Chem.* **1999**, *71*, 2192.
(59) Katz, E.; Willner, I. *Electroanalysis* **2003**, *15*, 913.
(60) Park, J.-Y.; Lee, Y-S; Kim, B. H.; Park, S.-M. *Anal. Chem.* **2008**, *80*, 4986.
(61) Sallacan, N.; Zayats, M.; Bourenko, T.; Kharitonov, A. B.; Willner, I. *Anal. Chem.* **2002**, *74*, 702.
(62) Fick, J.; Steitz, R.; Leiner, V.; Tokumitsu, S.; Himmelhaus, M.; Grunze, M. *Langmuir* **2004**, *20*, 3848.
(63) Katz, E.; Willner, I. *Electroanalysis* **2003**, *15*, 913.
(64) Fragoso, A.; Laboria, N.; Latta, D.; O'Sullivan, C. K. *Anal. Chem.* **2008**, *80*, 2556.
(65) Tummler, B.; Maass, G.; Vogtle, F.; Sieger, H.; Hei Mann, U.; Weber, E. *J. Am. Chem. Soc.* **1979**, *101*, 2588.
(66) Zeller, E. T.; Park, J.; Hsu, T.; Groves, W. A. *Anal. Chem.* **1998**, *70*, 4191.
(67) Albert, K. J; Walt, D. R. *Anal. Chem.* **2000**, *72*, 1947.
(68) Rammel, U.; Reinhard, G. *Electrochim. Acta* **1990**, *35*, 1045.
(69) Kerner, Z.; Pajkossy, T. *Electrochim. Acta* **2000**, *46*, 207.
(70) Pajkossy, T. *Solid State Ionics* **1997**, *94*, 123.